AGU
GC13A-1069
December 3, 2012

Future Flood Risk at NASA Ames Research Center (South San Francisco Bay)

William B Mills
Tetra Tech, Inc., Lafayette, CA, USA
bill.mills@tetratech.com

Mariza C Costa-Cabral
Hydrology Futures, LLC, Seattle, WA, USA
cabral@hydrologyfutures.com

Peter D Bromirski
Scripps Institution of Oceanography, La Jolla, CA, USA

Norman L Miller
Geography, U.C. Berkeley, Berkeley, CA, USA

Robert N Coats
Hydroikos Ltd., Berkeley, CA, USA

Max Loewenstein
NASA Ames Research Center, Moffett Field, CA, USA

Sujoy B Roy
Tetra Tech, Inc., Lafayette, CA, USA

Michael MacWilliams
Delta Modeling Associates, San Francisco, CA, USA

Josephine Fong
Mathematics U.C. Berkeley, Berkeley, CA, USA

INTRODUCTION

CLIMATE CHANGE AND FLOODING RISK AT NASA AMES

President Obama has mandated (E.O. 13514) that all federal agencies evaluate vulnerabilities of their mission, facilities and operations, to climate variability and change. Our project focuses on NASA Ames Research Center (NASA Ames) located in Silicon Valley, California (Figure 1). NASA Ames mission categories include supercomputing, intelligent systems, astrobiology, small satellites, robotic lunar exploration, nanotechnology, information technology, aviation, and others; employing about 2300 personnel and supporting more than 8400 jobs. Its current infrastructure alone is valued at over USD$3 billion and its annual economic output is about USD$1.3 billion. The new planned NASA Research Park is expected to generate nearly USD$6 billion in annual economic impact.

This poster focuses on our ongoing research on flooding risk at NASA Ames, as influenced by observed and projected climate change, especially in the following impacts:

(a) Sea level rise, amplifying the impacts of extreme high tides and storm surges.

(b) Impacts on wetlands' sediment accretion rates, relative sea level rise, and species habitat.

(c) Possible increases in the frequency and intensity of extreme storms.

Impacts (a), (b) and (c) are expressions of synoptic-scale changes in ocean-atmosphere conditions and circulation (Figure 2).

Figure 1: Location of the NASA Ames campus in South San Francisco Bay. The Moffett Air-field is in the foreground. Photo: NASA

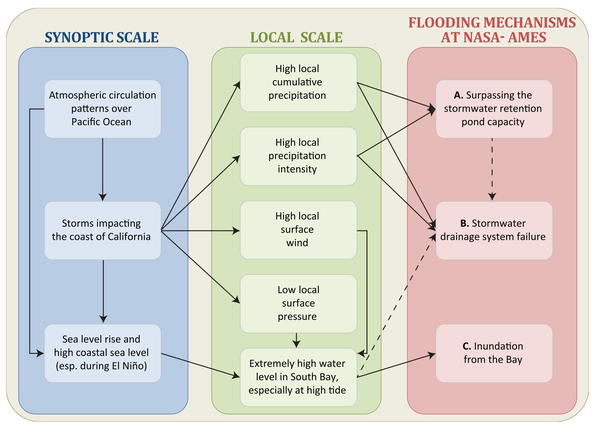

Figure 2: Cross-scale ocean-atmosphere conditions influencing flooding at NASA Ames. Dashed arrows indicate relationships (arrows) that presently require clarification.

Figure 3: Intense precipitation on February 3, 1998, preceded by a very wet winter, and accompanied by extreme high water levels in the South S.F. Bay, led to flooding at NASA Ames. Photo: NASA archives.

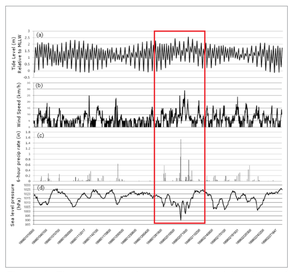

Figure 4: The unusual values measured at the time of flooding (pictured in Figure 3), for (a) total water height in the Bay, which includes large non-tidal residuals, (b) wind speed (high), (c) 6-hourly precipitation (high), and (d) sea level pressure (low). Figure modified from Burroughs (2009, from internship work at NASA Ames).

SEA LEVEL RISE PROJECTIONS AND MARSH ACCRETION

PROJECTED RELATIVE SEA LEVEL RISE

Major uncertainties persist associated with global and regional sea level rise projections. Knowles (2009), in a study that is widely used for planning purposes in S.F. Bay, estimated a rise of 1m by 2081 and 1.5m by 2105. More recently, the National Research Council (NRC 2012) published projections for California, Oregon and Washington, taking into account regional subsidence and uplift, as well as the contributions from thermal expansions of the oceans and melting of grounded glaciers and ice sheets. Figure 5 shows the low, medium, and high projections from the NRC report, and an estimate from Knowles (2009).

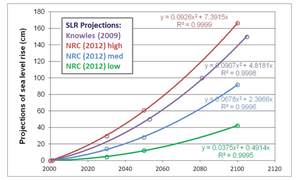

Figure 5: Sea level rise projections for S.F. Bay. All four curves are concave upward, and are well described by 2nd-order polynomials.

SEA LEVEL RISE AND SALT MARSH ACCRETION

Tidal wetlands at the edge of San Francisco Bay provide important services, including as buffers against wave erosion, protecting levees; habitat for endangered and threatened species (e.g., the California clapper rail and the salt marsh harvest mouse); and water quality protection, by pollutant (including heavy metals) adsorbing to sediment.

Here we investigate whether sediment deposition and plant growth in tidal marshes bordering NASA Ames have the potential to keep pace with projected sea level rise. At NASA Ames, tidal wetlands presently exist only along the edge of Stevens Creek, a realigned fully-tidal flood control channel. The western 54 ac of the Storm Water Retention Pond have, however been proposed for restoration as a tidal marsh (Brown & Caldwell 2005). Before the parcel is restored to tidal action, we must understand how sea level rise will affect sediment deposition and plant growth, and whether restored wetlands will keep pace with SLR. If the rate of SLR exceeds that of sediment accretion to the marsh surface, the wetlands will revert to tidal and ultimately subtidal mud flats (Figure 7). Using core data from a nearby marsh (Figure 8) together with a local mean tidal month, we ran a sediment deposition model and found the average concentration of suspended sediment (175 mg/l) that accounts for the observed sediment deposition. We then ran the model using a local tide at Stevens Creek and the derived concentration together with the NRC projections for 21st century sea level rise (SLR).

The results show that with low and intermediate rates of SLR (Figures 9a,b), marsh accretion will keep pace with SLR, and both high and low elevation marsh environments will persist beyond the end of the century; but with the highest SLR rate (Figure 9c), wetlands restored to tidal action and NASA-ARC will develop a low tidal marsh that will persist to the end of the century, but eventually drown as the SLR rate exceeds the marsh accretion rate.

Figure 6 represents the extent of inundation of the NASA Ames campus at MHHW, corresponding to a rise in sea level of 1.4m, and assuming failure of the protective levees.

Figure 6: Extent of inundation of the NASA Ames campus at MHHW corresponding to a rise in sea level of 1.4m, in the case of levee failure, estimated from ortophotography and LiDAR point cloud.

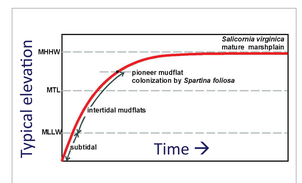

Figure 7: Typical evolution of a marsh plain due to deposition of sediment. Source: PWA and Faber, 2004.

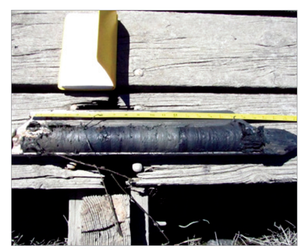

Figure 8: A sediment core from the Cooley Landing marsh, in the split core sampler. The bottom of the recent deposit is at about 17 in.

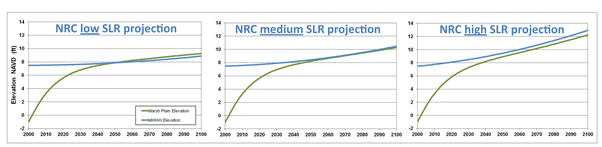

Figure 9: Simulated evolution of the elevation of the marsh plain, and of mean higher high water (MHHW) at NASA Ames, for the three sea level rise scenarios published by NRC (2012), designated low, medium and high.

REFERENCES

Brown & Caldwell (2005) Moffett Field Storm Water Retention Pond Tidal Restoration Feasibility Study. Report for NASA Ames Research Center.

PWA (Philip Williams & Associates, Ltd), Faber PM (2004) Design Guidelines for Tidal Wetland Restoration in San Francisco Bay. The Bay Institute and California State Coastal Conservancy, Oakland CA, 83 pp.

Knowles N (2009) Potential inundation due to rising sea levels in the San Francisco Bay region. California Climate Change Center CEC-500-2009-023-D. 21 pp.

National Research Council, Committee on Sea Level Rise in California, Oregon and Washington (2012) Sea level rise for the coasts of California, Oregon and Washington: Past, present and future. National Research Council. The National Academies Press, Washington DC. 250 pp.

CLIMATIC PROJECTIONS

DYNAMIC DOWNSCALING OF CLIMATE PROJECTIONS

We use NCAR's regional climate model Weather Research and Forecasting version 3 (WRF) coupled with the Community Land Model version 3.5 (Jin et al. 2010) to downscale the results of AOGCM climate runs for IPCC A1B scenario of greenhouse gas emissions (Nakicenovic et al. 2000) for 2060-2069, a time period when different emissions scenarios just begin to show departures in their climatic projections. Due to computational expense, we use the output of just two AOGCMs, the NCAR CCSM3 (Collins et al. 2006) and the GFDL CM2.1 (Delworth et al. 2006). The resulting dynamically downscaled 10-km resolution simulations are part of the California probabilistic projections program (Cayan et al. 2008; Miller et al. 2009; Pierce et al. 2012). The 10 km x 10 km resolution provides adequate definition of coastal California and San Francisco Bay as well as mountainous topography including the Sierra Nevada. The NASA Ames Research Center sub-domain is represented by 9 grid cells (900 km²).

Taylor diagrams (Taylor 2001) are used to quantify the similarity between two patterns, in this case the WRF runs forced by the AOGCM simulations against the WRF runs forced by the observational-based NCAR/NCEP Reanalysis II (NNR2: Kalnay et al. 1996). Figure 10 shows Taylor diagrams for ten-year averaged mean seasonal climatologies for different variables. Due to space limitations, only the winter season, DJF, is shown. As expected, **pressure** is very robust for the historical simulations (1985-1994). Bias analysis of downscaled **temperature** via CCSM/WRF and GFDL/WRF compared to NNR2/WRF (not shown) has correlation coefficients ranging from 0.5 to 0.8 for CCSM/WRF and 0.1 to 0.8 for CM2.1/WRF. Similarly, the **precipitation** correlation coefficient ranges from less than 0.1 in winter (DJF) to 0.6 in spring (MAM). Testing the historical accuracy of 10m height surface winds within the WRF code in the same fashion indicates that the **U-wind** magnitude correlates fairly well with coefficients near 0.8 during MAM, 0.6-0.7 (SON), 0.5-0.75 (JJA) and 0.35-0.45 (DJF). The **V-wind** component is less robust, with correlation coefficients 0.3-0.35 (MAM), 0.7-0.8 (JJA), 0.3-0.4 (SON) and <0.2 (DJF). Finally, the Taylor diagram analysis for climatological **soil moisture content** (not shown) indicates correlation coefficients between 0.7 and 0.95, suggesting a robust result.

Climate sensitivity indicates the difference, or percent change, between the 2060-2069 and 1985-1994 mean season climatologies. Figure 11 shows bar charts of seasonal-mean climatological sensitivites. Sensitivity is less clear for precipitation than for temperature, with (for DJF) a 10% reduction for CCSM/WRF and a 0.5% increase for GFDL/WRF. Both U and V wind magnitudes climatologically decrease during DJF, but the GFDL/WRF shows an increase during MAM.

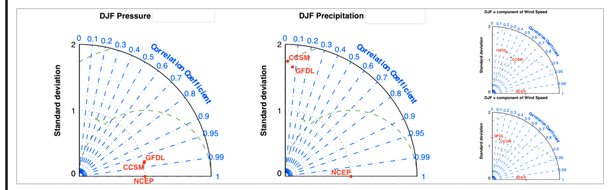

Figure 10: Taylor diagrams for winter season (DJF) for the NASA Ames region, comparing the accuracy of dynamically downscaled variables from CCSM/WRF and GFDL CM2.1/WRF to NCEP/WRF.

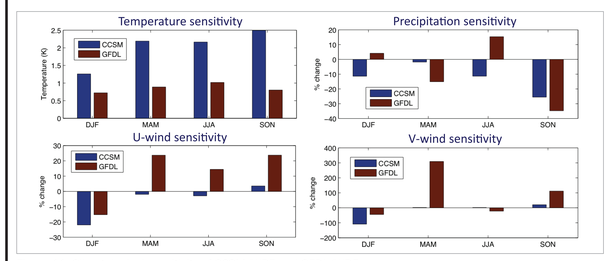

Figure 11: Climatological sensitivity of CCSM/WRF and GFDL/WRF.

Most relevant to this project is the daily time-series analysis of precipitation, sea level pressure and winds, as these are drivers for storm surge and flooding in this low-lying region. Evaluation of the percent change in daily and 3-day precipitation does not show significant changes (Figure 12). The U-wind slackens and V-wind does not change on the daily time scale. Nevertheless, other studies have obtained increases in projected precipitation intensity for this region (e.g. Pierce et al. 2012).

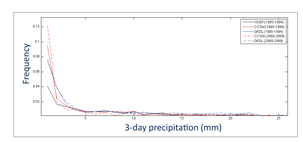

Figure 12: Distribution of 3-day precipitation, for observations (NCEP, 1985-1994), and the historical simulations and projections.

REFERENCES

Cayan D.R., E.P. Maurer, M.D. Dettinger, M. Tyree and K. Hayhoe (2008), Climate change scenarios for the California region, Climatic Change, 87, Suppl. 1: 21–42 doi: 10.1007/s10584-007-9377-6.

Collins, W. D. and Coauthors (2006), The formulation of the NCAR Community System Model version 3 (CCSM3), J. Climate, 19: 2122–2143.

Delworth, T.L., and Coauthors (2006), GFDL's CM2 global coupled climate models. Part I: Formulation and simulation characteristics. J. Climate, 19: 643–674.

Jin, J., N. L. Miller, and N. Schegel, 2010: Sensitivity Study of Four Land Surface Schemes in the WRF Model. Advances in Meteorology, DOI:10.1155/2010/167436.

Kalnay, E., M. Kanamitsu, R. Kistler, W. Collins, D. Deaven, L. Gandin, M. Iredell, S. Saha, G. White, J. Woollen, Y. Zhu, A. Leetmaa, and R. Reynolds (1996), The NCEP/NCAR 40-Year Reanalysis Project, Bull. Am. Meteorol. Soc., 77: 437–471.

Miller, N.L., J. Jin, N.J. Schlegel, D.R. Cayan, H. Hidalgo, M. Kanamitsu, H. Kanamaru, K. Yoshimira, P.B. Duffy, T. O'Brien, M. A. Synder, L.C. Sloan. (2009) An evaluation of simulated California climate using multiple dynamical and statistical downscaling techniques. CA Energy Comm. Rep. CEC-500-2008, 49pp.

Nakicenovic, N., Alcamo, J., Davis, G., de Vries, B., Fenhann, J., Gaffin, S., Gregory, K., Grübler, A. (2000), Special Report on Emissions Scenarios, Working Group III, Intergovernmental Panel on Climate Change (IPCC), Cambridge University Press, Cambridge, UK, 595(ISBN0521804930) (http://www.grida.no/climate/ipcc/ emission/index.htm).

Pierce, D. W., T. Das, D. R. Cayan, E. P. Maurer, N. L. Miller, Y. Bao, M. Kanamitsu, K. Yoshimura, M. A. Snyder, L. C. Sloan, G. Franco, M. Tyree, 2012: Probabilistic estimates of future changes in California temperature and precipitation using statistical and dynamical downscaling. Climate Dynamics, doi 10.1007/s00382-012-1337-9.

Skamarock, W. C., J. B. Klemp, J. Dudhia, D. O. Gill, D. M. Barker, W. Wang, and J. G. Powers, (2005), A Description of the Advanced Research WRF Version 2, NCAR Tech Note, NCAR/TN—468+STR, 88.

Solomon Ed. S., D. Qin, M. Manning, Z. Chen, M. Marquis, K. B. Avery, M. Tignor, and H. L. Miller, IPCC, (2007): Summary for Policymakers. In: Climate Change 2007: The Physical Basis. Contribution of Working Group I to the Fourth Assessment Report of the Intergovernmental Panel on Climate Change. Cambridge, UK: Cambridge University Press.

Taylor, K.E. Taylor, K.E.: Summarizing multiple aspects of model performance in a single diagram. J. Geophys. Res., 106, 7183-7192, 2001 (also see PCMDI Report 55, http://www.pcmdi.llnl.gov/publications/ab55.html).

STATISTICAL MODELS OF EXTREMES

STATISTICAL DOWNSCALING OF PRECIPITATION EXTREMES AND EXTREME NON-TIDAL WATER HEIGHT IN SOUTH S.F. BAY

Each of these two variables – extreme precipitation, and extreme non-tidal water height in South S.F. Bay – can be modeled with a Generalized Extreme Value (GEV) distribution. We incorporate predictor variables into each GEV distribution, by expressing the location and scale parameters as (linear) functions of the predictors (e.g. Smith 1989; Coles 2001; Katz et al. 2002; Wang and Zhang 2008; Zhang et al. 2010). This work is in progress. The goal is to obtain estimates of precipitation extremes for NASA Ames from variables that are simulated by AOGCM/RCM climate models (see the panel to the left) with greater reliability than extreme precipitation can currently be simulated. Statistical downscaling requires that there exist predictor variables with significant influence on the predictand variable, and that the statistical regression model that relates predictors to a predictand is identified and parameterized correctly. It also requires the assumption that observed relationships (regression models) will still hold in an altered future climate – which represents a source of uncertainty. We are investigating candidates for predictor variables for our two predictands. We are interested in predictor variables that reflect (see Figure 2): a) large-scale conditions, and b) local storms. Some possibilities are explored below. This approach has the benefit of providing an analytical basis for calculation of the joint probability of extremes of the two variables, on the basis of AOGCM/RCM projections of large-scale conditions and local storms, whose predictor variables determine the parameter values of both extreme value distributions.

PREDICTORS DESCRIBING LARGE-SCALE CONDITIONS

Figure 13 shows the computed correlation between climate indices and precipitation at NASA Ames (Moffett Field station). We consider total precipitation in a water year (left), and the 5-day precipitation maximum (right). Nine climate indices are studied, and we show the correlation that is obtained with precipitation, depending on the month the index was measured (x axis). This ranges from the previous January (long lead time) to the end of the wet season (April). Absolute values smaller than 0.25 are not significant for our sample size of 67 years (this daily precipitation time series covers 1946-2012). Figure 13 shows that the largest correlations (in absolute value) are those for the NOI (Northern Oscillation Index) for Dec-Mar. Figure 14 shows NOI-precipitation correlation values for North America precipitation in DJFM. The large-scale predictors that we seek may be rotated principal components of climate indices.

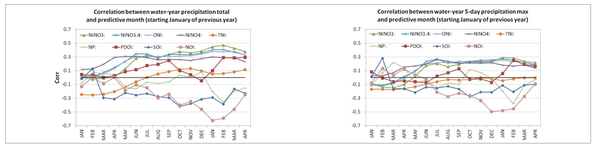

Figure 13: Predictive ability of different climate indices at variable lead times (from January of the previous year through the end of the wet season in April), for total water-year precipitation (left) and maximum 5-day precipitation (right). Based on daily precipitation records from the Moffett Field meteorological station. Climate indices data downloaded from http://www.esrl.noaa.gov/psd/data/climateindices/list/.

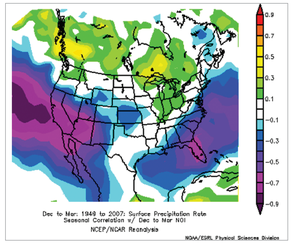

Figure 14: Correlation between the NOI and seasonal precipitation (Dec-Mar) in 1949-2007. NOAA's correlation web page (www.esrl.noaa.gov/psd/data/correlation) was used to produce this figure.

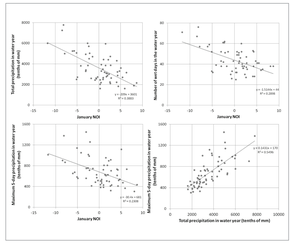

Figure 15: January value of the NOI as a predictor of a) total water-year precipitation, b) number of wet days, and c) maximum 5-day precipitation. d) Water years with high precipitation totals tend to experience more intense precipitation episodes, e.g. 5-day totals.

PREDICTORS DESCRIBING LOCAL STORM CONDITIONS

Wang and Zhang (2008) used gridded sea level pressure (SLP) to represent flow patterns and storminess that influence precipitation. Wilby and Wigley (2000) showed that the maximum correlation between SLP and precipitation is obtained for SLP measured at a distance from the precipitation station. Similar behavior may be true for extreme water heights. In addition to SLP, Wang and Zhang (2008) also used humidity at the 850-hPa level, measured at the station location.

PROPAGATION OF EXTREME NON-TIDAL WATER HEIGHT INTO SOUTH SAN FRANCISCO BAY

The statistical model described above will permit development of a statistical distribution for the extremes of water height, in the form of a GEV, whose parameters are obtained by regression using predictor variables of large-scale conditions (climate indices or their principal components) and local storminess (SLP and humidity). This GEV will describe the frequency and intensity of extreme water heights at San Francisco. The propagation of those disturbances into the South S.F. Bay, which may cause extreme water heights at NASA Ames, is complex to simulate. We hope to make use of the UnTRIM (3-D) hydrodynamic model of S.F. Bay to simulate this propagation (e.g. MacWilliams et al., 2012). Even without a future increase in storminess (see Bromirski et al. 2012), sea level rise will increase the severity of storms' impacts, and the scenarios represented in Figure 5 will be considered.

REFERENCES

Bromirski PD, Cayan DR, Graham N, Tyree M, Flick RE (2012) Coastal flooding-potential projections: 2000-2100, Public Interest Energy Res. Program White Paper CEC-500-2012-011, 39 pp, Scripps Inst. Of Oceanogr. La Jolla CA.

Coles S (2001) An Introduction to Statistical Modeling of Extreme Values. Springer-Verlag, 208pp.

Smith RL (1989) Extreme value analysis of environmental time series: An application to trend detection in ground-level ozone (with discussion). Stat Sci 4:367-393.

Katz RW, Parlange MB, Naveau P (2002) Statistics of extremes in hydrology. Adv Water Resour 23:133-139.

MacWilliams ML, Kilham NE, Bever AB (2012) South San Francisco Bay Long Wave Modeling Report, South San Francisco Bay Shoreline Study. Prepared for the US Army Corps of Engineers, San Francisco District, June 30, 2012, 172 pp.

Wang J, Zhang X (2008) Downscaling and projection of winter extreme daily precipitation over North America. J Clim:923-937.

Wilby RL, Wigley TML (2000) Precipitation predictors for downscaling: Observed and general circulation model relationships. Int J Climatol 20:641-661.

Zhang X, Wang J, Zwiers FW, Groisman PY (2010) The influence of large-scale climate variability on winter maximum daily precipitation over North America. J Clim 23.

**This material is based upon work supported by NASA under award No NNX12AG33G. Any opinions, findings, and conclusions or recommendtions expressed in this material are those of the authors and do not necessarily reflect the views of the National Aeronautics and Space Administration.